Electronic Supplementary Information for Dalton Transactions

Manisyl-substituted polypyridine coordination compounds: Metallo-supramolecular networks of interdigitated double helices assembled via π–π interactions

Jeremy K. Klosterman, Anthony Linden, Derick K. Frantz and Jay S. Siegel*

Supporting Information:

Section

A) NMR Spectroscopy

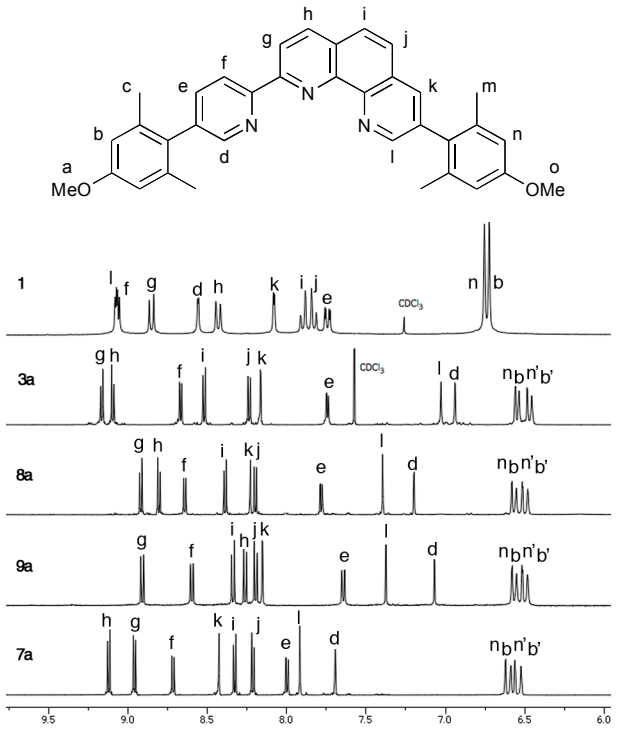

Fig. S1 Aromatic region of ^{1}H NMR spectra of **1** in $CDCl_3$ and M(pherpy)$_2$-2PF$_6$ complexes **3a**, **7a** –**9a** in CD_3CN.

Table S1. 600 MHz ^{1}H NMR chemical shifts of **1** in $CDCl_3$ and diamagnetic M(pherpy)$_2$-2PF$_6$ complexes **3a**, **7a** – **9a** in CD_3CN.

	b/b'	c/c'	d	e	f	g	h	i	j	k	l	m/m'	n/n'
1[a]	6.73	2.10	8.56	7.74	9.06	8.86	8.43	7.90	7.83	8.08	9.07	2.08	6.76
3a	6.54, 6.46	1.49, 1.19	6.94	7.74	8.67	9.16	9.10	8.52	8.24	8.16	7.03	1.48, 1.20	6.56, 6.48
6a	6.55, 6.48	1.57, 1.33	7.20	7.78	8.64	8.92	8.80	8.39	8.20	8.23	7.40	1.57, 1.36	6.58, 6.52
7a	6.55, 6.48	1.58, 1.38	7.07	7.65	8.60	8.91	8.27	8.34	8.20	8.16	7.38	1.57, 1.36	6.58, 6.51
5a	6.59, 6.53	1.67, 1.48	7.70	8.00	8.72	8.96	9.12	8.33	8.21	8.43	7.92	1.66, 1.45	6.62, 6.56

[a] In $CDCl_3$.

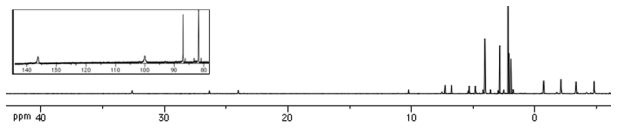

Fig. S2 600 MHz ^{1}H NMR spectrum of a CD_3CN solution of **4a** Co(pherpy)$_2$-2PF$_6$.

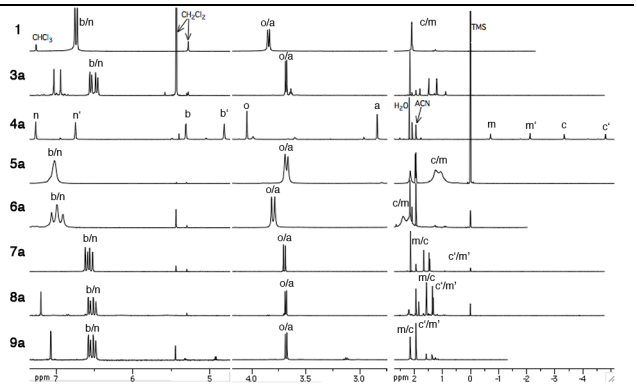

Fig. S3 Manisyl region of the ^{1}H NMR spectra of M(pherpy)$_2$-2PF$_6$ complexes **3a** – **9a** (in CD_3CN).

Table S2 600 MHz ^{1}H NMR chemical shifts of manisyl protons in CD_3CN solutions of M(pherpy)$_2$-2PF$_6$ complexes **3a** – **9a**

		a	b/b'	c/c'	m/m'	n/n'	o
1[a]		3.84	6.73	2.10	2.08	6.76	3.87
3a	Fe(II)	3.68	6.54, 6.46	1.49, 1.19	1.48, 1.20	6.56, 6.48	3.69
4a	Co(II)	2.84	5.31, 4.81	-3.34, -4.81	-0.71, -2.12	7.27, 6.75	4.20
5a	Ni(II)	3.67	7.02	1.06	1.25	7.02	3.69
6a	Cu(II)	3.79	6.99, 6.91	2.01	2.39	7.06, 6.99	3.82
7a	Zn(II)	3.69	6.59, 6.53	1.67, 1.48	1.66, 1.45	6.62, 6.56	3.71
8a	Ru(II)	3.68	6.55, 6.48	1.57, 1.33	1.57, 1.36	6.58, 6.52	3.69
9a	Os(II)	3.67	6.55, 6.48	1.58, 1.38	1.57, 1.36	6.58, 6.51	3.69

[a] In $CDCl_3$

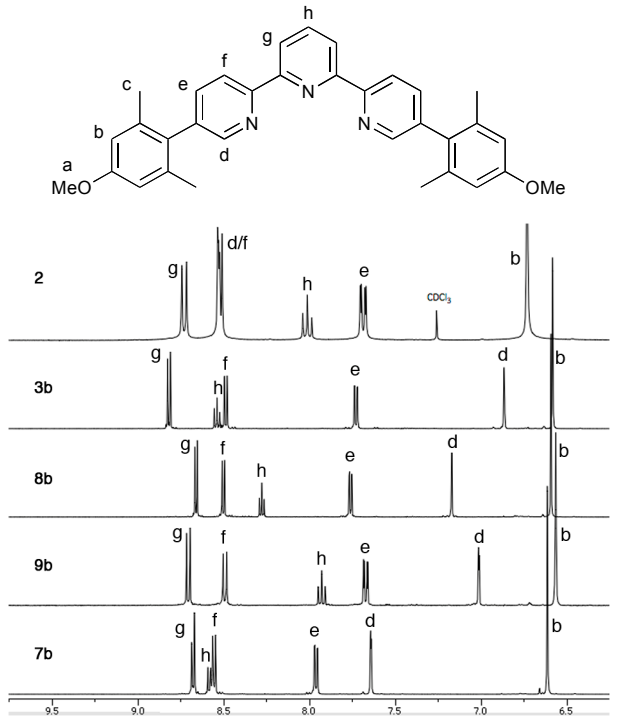

Fig. S4 Aromatic region of ^{1}H NMR spectra of **2** in $CDCl_3$ and diamagnetic M(terpy)$_2$-2PF$_6$ complexes **3b**, **7b** –**9b** in CD_3CN

Table S3 600 MHz ^{1}H NMR chemical shifts of **2** in $CDCl_3$ and diamagnetic M(terpy)$_2$-2PF$_6$ complexes **3b**, **7b** – **9b** in CD_3CN

		a	b	c	d	e	f	g	h
2[a]		3.85	6.73	2.09	8.52	7.68	8.51	8.72	8.01
3b	Fe(II)	3.72	6.58	1.49	6.86	7.73	8.49	8.82	8.55
8b	Ru(II)	3.72	6.59	1.57	7.17	7.76	8.50	8.66	8.28
9b	Os(II)	3.72	6.57	1.62	7.01	7.67	8.49	8.71	7.93
7b	Zn(II)	3.72	6.62	1.63	7.64	7.96	8.56	8.68	8.58

[a] In $CDCl_3$

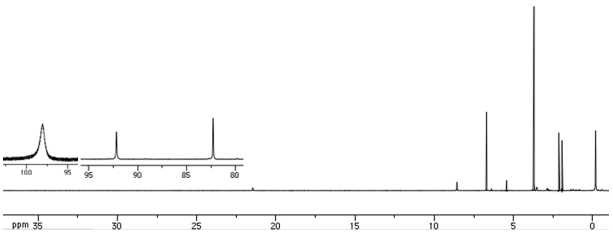

Fig. S5 600 MHz ^{1}H NMR spectrum of a CD_3CN solution of **4b** Co(terpy)$_2$-2PF$_6$.

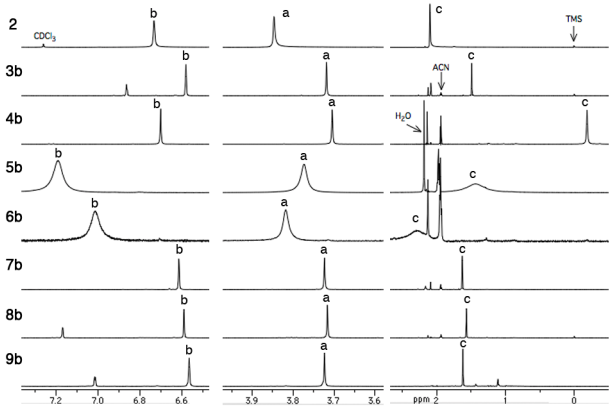

Fig. S6 Manisyl region of the ^{1}H NMR spectra of CD_3CN solutions of M(terpy)$_2$-2PF$_6$ complexes **3b** – **9b**.

Table S4 600 MHz ^{1}H NMR chemical shifts of manisyl protons in CD_3CN solutions of M(terpy)$_2$-2PF$_6$ complexes **3b** – **9b**.

		a	b	c
2[a]		3.85	6.73	2.09
3b	Fe(II)	3.72	6.58	1.49
4b	Co(II)	3.71	6.7	-0.18
5b	Ni(II)	3.74	7.14	1.42
6b	Cu(II)	3.81	7.01	2.27
7b	Zn(II)	3.72	6.62	1.63
8b	Ru(II)	3.72	6.59	1.57
9b	Os(II)	3.72	6.57	1.62

[a] In $CDCl_3$.

B) X-ray Crystallography

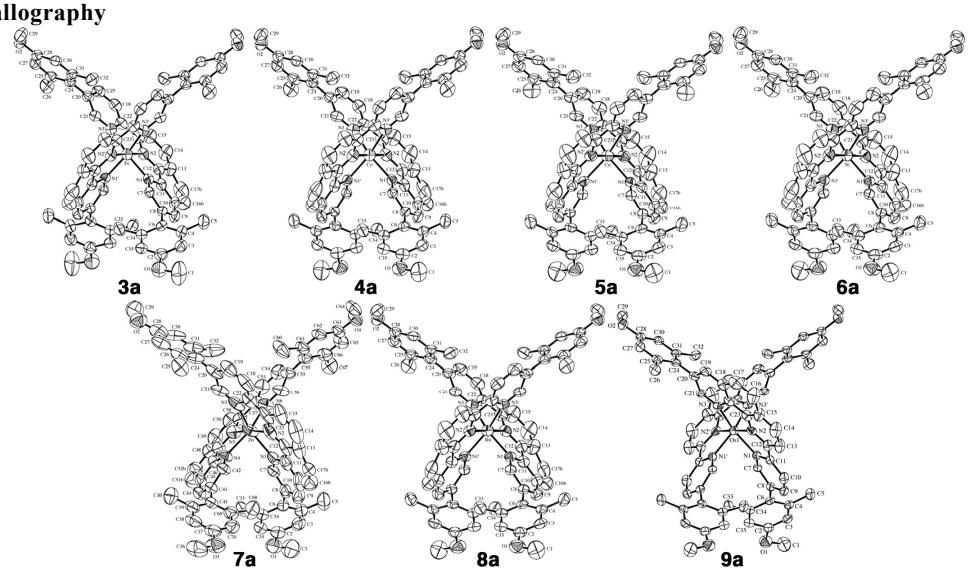

Fig. S7 ORTEPs of M(pherpy)$_2$-PF$_6$ complexes **3a** – **9a** with hydrogen atoms, counter-ions, and solvent molecules removed for clarity

Table S5 Crystallographic data for pyridyl-phenanthroline complexes **3a** – **9a**

	3a	**4a**	**5a**	**6a**	**7a**	**8a**	**9a**
Formula	Fe(pherpy)$_2$ •2PF$_6$•2CH$_3$CN	Co(pherpy)$_2$ •2PF$_6$•2CH$_3$CN	Ni(pherpy)$_2$ •2PF$_6$•2CH$_3$CN	Cu(pherpy)$_2$ •2PF$_6$•2CH$_3$CN	Zn(pherpy)$_2$ •2PF$_6$•3CH$_3$CN	Ru(pherpy)$_2$ •2PF$_6$•2CH$_3$CN	Os(pherpy)$_2$ •2PF$_6$•2CH$_3$CN
Formula weight	1479.17	1482.26	1482.03	1486.87	1529.76	1524.33	1613.53
Color	Purple	Orange-brown	Yellow	Lime-green	Light yellow	Red	Purple-brown
Crystal system	orthorhombic	orthorhombic	orthorhombic	orthorhombic	monoclinic	orthorhombic	orthorhombic
Space group	*Pcca*	*Pcca*	*Pcca*	*Pcca*	$P2_1/c$	*Pcca*	*Pcca*
Z	4	4	4	4	4	4	4
a [Å]	25.6038(5)	25.3072(4)	25.3094(4)	24.9866(3)	12.9177(1)	25.3777(5)	25.3861(5)
b [Å]	12.2125(2)	12.5642(1)	12.6402(2)	12.9263(2)	25.4666(3)	12.5601(3)	12.5157(3)
c [Å]	21.8379(3)	21.8238(3)	21.9538(3)	21.9263(3)	22.1526(3)	21.8678(4)	21.8136(4)
α [º]	90	90	90	90	90	90	90
β [º]	90	90	90	90	93.0097(8)	90	90
γ [º]	90	90	90	90	90	90	90
V[Å^3]	6828.4(2)	6939.2(2)	7023.4(2)	7081.9(2)	7277.5(1)	6970.3(3)	6930.7(2)

Table S6 Selected bond lengths (Å), atomic distances (Å), and angles (deg) of pyridyl-phenanthroline complexes **3a** – **9a**

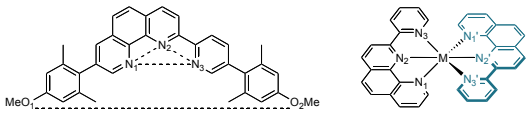

	3a	**4a**	**5a**	**6a**	**7a**	**8a**	**9a**
Metal	Fe(II)	Co(II)	Ni(II)	Cu(II)	Zn(II)[a]	Ru(II)	Os(II)
Space group	*Pcca*	*Pcca*	*Pcca*	*Pcca*	$P2_1/c$	*Pcca*	*Pcca*
M-N(1)	2.002(3)	2.086(3)	2.127(3)	2.186(3)	2.255(6)/2.196(5)	2.084(4)	2.088(7)
M-N(2)	1.878(3)	1.879(3)	1.968(3)	1.937(3)	2.045(6)/2.032(5)	1.978(4)	1.980(6)
M-N(3)	2.012(3)	2.105(3)	2.135(3)	2.198(3)	2.206(7)/2.211(5)	2.096(4)	2.077(7)
N(1)-M-N(3)[º]	161.2(1)	160.0(1)	156.6(1)	156.8(1)	152.8(2)/152.9(2)	157.4(2)	157.4(3)
N(1)-N(2)-N(3)[º]	103.9(1)	107.5(1)	107.3(1)	110.3(1)	109.9(3)/109.4(3)	105.2(2)	104.8(3)
N(1)···N(3)	3.961(4)	4.127(4)	4.173(4)	4.294(4)	4.336(8)/4.285(8)	4.099(5)	4.08(1)
O(1)···O(2)	16.811(4)	17.074(4)	17.091(5)	17.247(5)	17.446(9)/17.184(8)	17.010(7)	16.95(1)
O(1)···O(1')	12.848(5)	12.574(5)	12.502(5)	12.293(5)	12.56(1)	12.521(7)	12.54(1)
O(1)···O(2')	15.761(4)	15.895(4)	15.799(5)	15.888(5)	16.038(8)	15.780(7)	15.72(1)
O(2)···O(1')	15.761(4)	15.895(4)	15.799(5)	15.888(5)	15.347(9)	15.780(7)	15.72(1)
O(2)···O(2')	13.133(4)	13.105(4)	13.190(4)	13.168(4)	13.221(8)	13.183(6)	13.156(9)
N(2)-M-N(2')[º]	179.0(2)	179.2(2)	178.7(2)	179.1(2)	171.3(3)	179.3(2)	178.6(4)
Θ [º]	84.1(2)	83.6(2)	83.5(2)	83.0(2)	83.9(3)	82.6(2)	82.0(4)

[a] The two ligands are non-equivalent

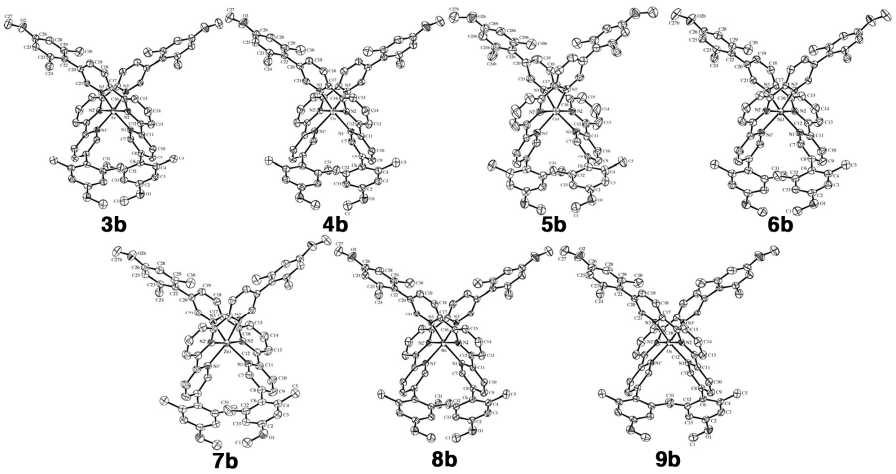

Fig. S7 ORTEPs of $M(terpy)_2$-PF_6 complexes **3b** – **9b** with hydrogen atoms, counter-ions, and solvent molecules removed for clarity

Table S7 Crystallographic data for terpyridine complexes **3b** – **9b**

	3b	**4b**	**5b**	**6b**	**7b**	**8b**	**9b**
Formula	$Fe(terpy)_2$-$2PF_6$-$6CH_3CN$	$Co(terpy)_2$-$2PF_6$-$6CH_3CN$	$Ni(terpy)_2$-$2PF_6$-$3CH_3CN$	$Cu(terpy)_2$-$2PF_6$-$2.5CH_3CN$	$Zn(terpy)_2$-$2PF_6$-$2.82CH_3CN$	$Ru(terpy)_2$-$2PF_6$-$6CH_3CN$	$Os(terpy)_2$-$2PF_6$-$6CH_3CN$
Formula weight	1595.33	1598.43	1475.04	1459.35	1474.46	1640.49	1729.69
Color	red	red	orange	green	colorless	red	brown
Crystal system	monoclinic	monoclinic	orthorhombic	orthorhombic	orthorhombic	monoclinic	monoclinic
Space group	*C*2/*c*	*C*2/*c*	*Pnna*	*Pnna*	*Pnna*	*C*2/*c*	*C*2/*c*
Z	4	4	8	8	8	4	4
a [Å]	29.749(1)	29.5268(4)	22.0069(3)	22.0072(3)	22.0637(2)	29.4883(4)	29.4529(4)
b [Å]	11.4106(4)	11.7893(3)	25.2020(5)	24.9787(4)	25.1063(4)	11.8087(1)	11.8271(1)
c [Å]	22.7396(6)	22.4187(5)	24.8731(3)	25.1014(3)	25.1199(4)	22.4060(3)	22.4142(2)
α [º]	90	90	90	90	90	90	90
β [º]	90.062(2)	90.847(2)	90	90	90	90.9353(6)	90.9746(7)
γ [º]	90	90	90	90	90	90	90
V[Å^3]	7719.1(4)	7803.1(3)	13795.1(4)	13798.5(3)	13914.9(3)	7801.1(2)	7806.7(1)

Table S8 Selected bond lengths (Å), atomic distances (Å), and angles (deg) of terpyridine complexes **3b** – **9b**

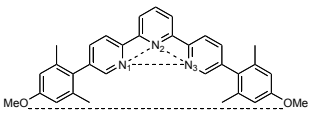

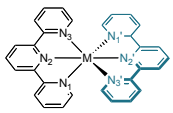

	3b	**4b**	**5b***		**6b***		**7b***		**8b**	**9b**
Metal	Fe(II)	Co(II)	Ni(II)		Cu(II)		Zn(II)[a]		Ru(II)	Os(II)
Space group	*C*2/*c*	*C*2/*c*	*Pnna*		*Pnna*		*Pnna*		*C*2/*c*	*C*2/*c*
M-N(1)	1.975(2)	2.063(2)	2.122(3)	2.107(3)	2.177(4)	2.161(4)	2.186(4)	2.159(4)	2.060(2)	1.984(2)
M-N(2)	1.878(2)	1.882(2)	1.983(3)	1.995(3)	1.964(4)	1.975(4)	2.061(4)	2.074(4)	1.972(2)	2.058(2)
M-N(3)	1.971(2)	2.057(2)	2.113(3)	2.114(3)	2.167(4)	2.159(4)	2.170(4)	2.183(4)	2.060(2)	2.062(2)
N(1)-M-N(3)[º]	162.12(8)	160.92(9)	156.3(1)	156.3(1)	156.2(2)	155.8(2)	152.3(2)	151.7(2)	158.73(6)	157.94(9)
N(1)-N(2)-N(3)[º]	102.2(1)	105.7(1)	106.4(1)	105.8(1)	108.9(2)	108.4(2)	107.7(2)	107.5(2)	103.63(7)	103.7(1)
N(1)···N(3)	3.899(3)	4.063(3)	4.146(4)	4.131(4)	4.251(6)	4.223(6)	4.230(6)	4.210(6)	4.049(2)	4.044(3)
O(1)···O(2)	16.770(3)	16.952(3)	17.50(1)	17.04(4)	17.59(2)	16.96(2)	17.50(2)	16.98(3)	16.861(3)	16.830(3)
O(1)···O(1')	13.591(3)	13.465(3)	13.632(3)	12.859(4)	13.724(6)	12.808(6)	13.766(5)	12.928(5)	13.505(2)	13.516(3)
O(1)···O(2')	15.297(3)	15.405(3)	15.64(1)	15.57(4)	15.72(2)	15.49(2)	15.53(2)	15.43(3)	15.343(3)	15.341(3)
O(2)···O(2')	13.864(3)	13.769(3)	12.38(2)	13.56(4)	12.24(2)	13.72(2)	12.33(2)	13.47(3)	13.682(3)	13.618(4)
N(2)-M-N(2')[º]	179.8(1)	179.4(1)	178.7(2)	176.9(2)	178.6(2)	176.2(2)	177.9(2)	175.1(2)	179.34(9)	179.4(1)
Θ [º]	86.1(1)	85.5(1)	84.8(2)	83.5(2)	85.0(2)	82.8(2)	84.6(2)	83.3(2)	84.39(9)	83.9(1)

* contains two, symmetry-independent, cations

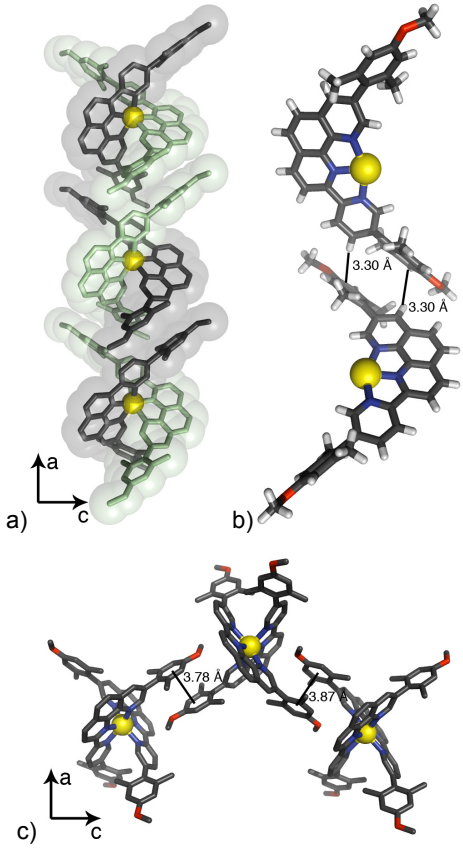

Fig. S8 Crystal packing of Zn(pherpy)$_2$-2PF$_6$ **7a** highlighting a) the stacking of dications to form a right-handed double helix, b) the intra-molecular C-H···π interactions between adjacent ligands within a single strand of the double helix and c) intra-strand π-stacking perpendicular to the helical axis.

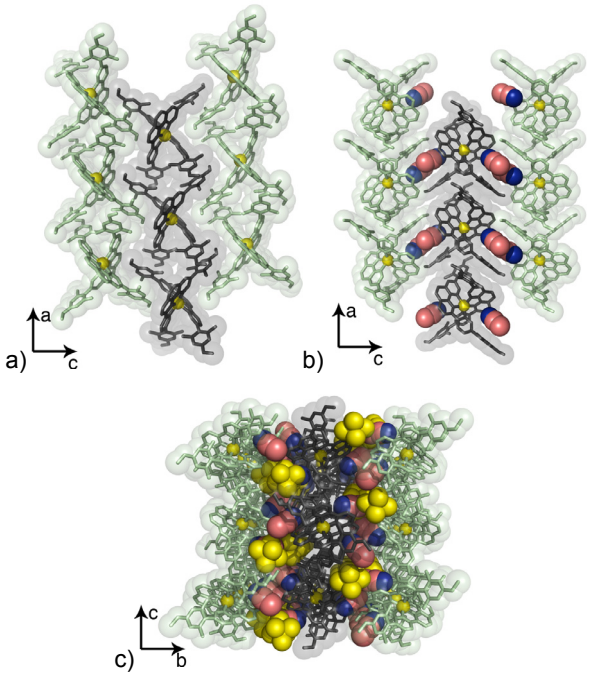

Fig. S9 Crystal packing structure of Zn(pherpy)$_2$-2PF$_6$ **7a** showing a) the 2D sheet of alternating double-helices along the b axis, b) the side view of the sheets along the c axis, and c) the top view of the sheets along the a axis

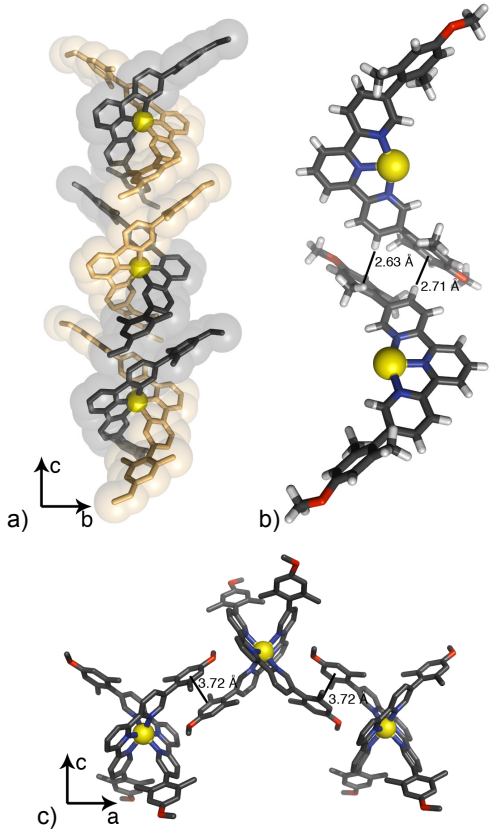

Fig. S10 Crystal packing of Zn(terpy)$_2$-2PF$_6$ **7b** showing a) the stacking of dications to form a right-handed double helix, b) the intra-molecular C-H···π interactions between adjacent ligands within a single strand of the double helix and c) intra-strand π-stacking perpendicular to the helical axis.

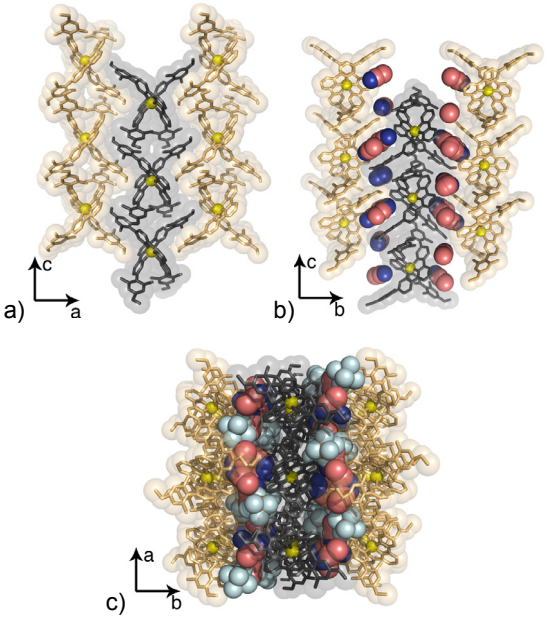

Fig. S11 Crystal packing structure of Zn(terpy)$_2$-2PF$_6$ **7b** highlighting a) the 2D sheet of alternating double-helices along the b axis, b) the side view of the sheets along the a axis, and c) the top view of the sheets along the c axis

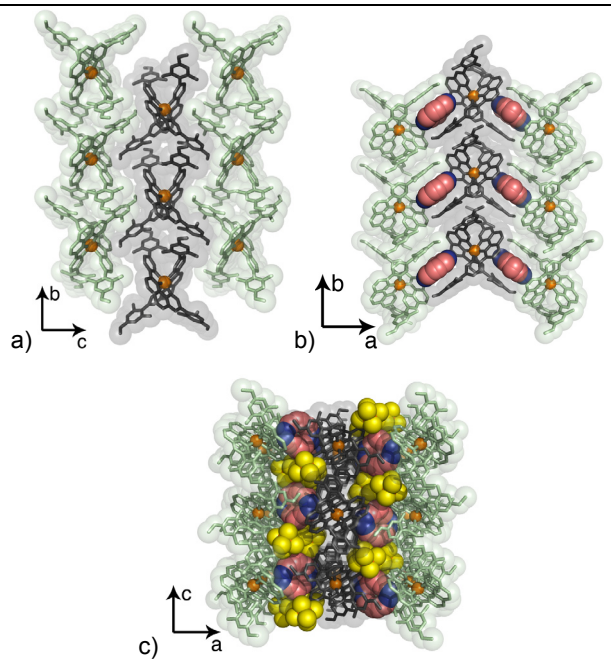

Fig. S12 Crystal packing structure of of Ru-doped $Zn(pherpy)_2$-$2PF_6$ crystals showing a) the 2D sheet of alternating double-helices along the b axis, b) the top view of the sheets along the a axis and c) the side view of the sheets along the b axis.

Table S9 Crystallographic data for pyridyl-phenanthroline complexes **7a**, **8a**, and the **40:1** mixed crystal

Formula	$Zn(pherpy)_2$-$2PF_6$-$3CH_3CN$	$Ru(pherpy)_2$-$2PF_6$-$2CH_3CN$	$Zn(pherpy)_2$-$2PF_6$-$2CH_3CN$
Formula weight	1529.76	1524.33	1488.71
Color	Light yellow	Red	Red-orange
Crystal system	monoclinic	orthorhombic	orthorhombic
Space group	$P2_1/c$	*Pcca*	*Pcca*
Z	4	4	4
a [Å]	12.9177(1)	25.3777(5)	24.974(1)
b [Å]	25.4666(3)	12.5601(3)	12.912(1)
c [Å]	22.1526(3)	21.8678(4)	22.066(1)
α [°]	90	90	90
β [°]	93.0097(8)	90	90
γ [°]	90	90	90
V[Å^3]	7277.5(1)	6970.3(3)	7115.5(7)

C) UV-Vis Spectroscopy

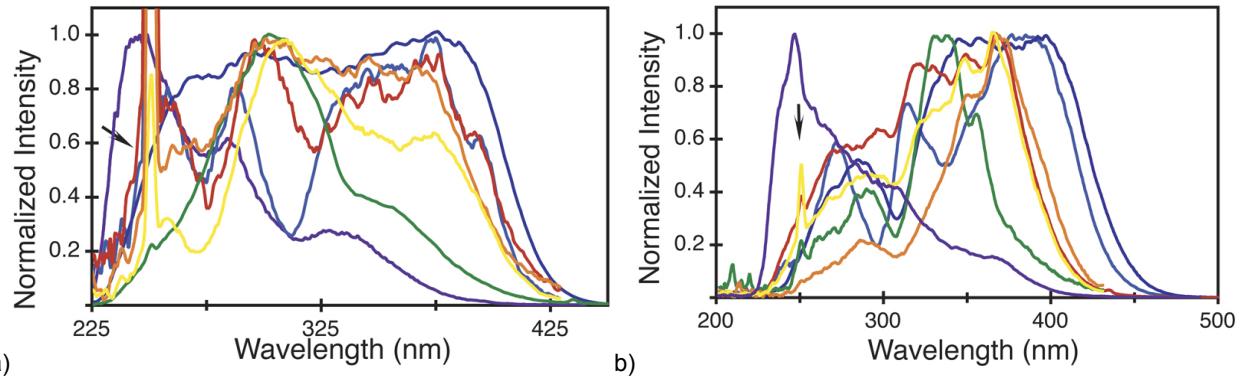

Fig. S13 Normalized excitation spectra of (a) M(pherpy)$_2$-2PF$_6$ complexes **3**a– **9a** and (b) M(terpy)$_2$ -2PF$_6$ complexes **3b** – **9b** in CH_2Cl_2: Fe(L)$_2$-2PF$_6$ (-red-), Co(L)$_2$-2PF$_6$ (-orange-), Ni(L)$_2$-2PF$_6$ (-yellow-), Cu(L)$_2$-2PF$_6$ (-green-), Zn(L)$_2$-2PF$_6$ (-blue-), Ru(L)$_2$-2PF$_6$ (-indigo-), Os(L)$_2$-2PF$_6$ (-violet-).

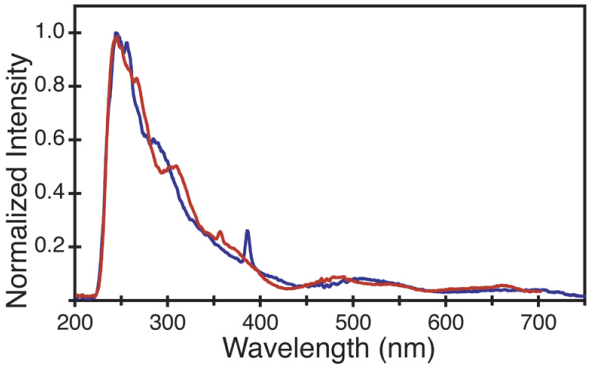

Fig. S14 Normalized excitation spectra of Os(pherpy)$_2$-2PF$_6$ **9a** (-blue-) and Os(terpy)$_2$-2PF$_6$ **9b** (-red-) in CH_2Cl_2

Table S11 UV-Vis absorption properties of M(terpy)$_2$-2PF$_6$ complexes **3b** – **9b** in methylene chloride

	λ_{max} (nm)	ε_{max}	$\lambda_{maxMLCT}$ (nm)	$\varepsilon_{maxMLCT}$
2	287*, 305	27800		
3b	275*, 319, 351	59000	495sh, 555, 610sh	10000
4b	274*, 313, 335sh	52000	503, 553	1000
5b	271*, 345	75000		
6b	285sh*, 326	45000		
7b	279*, 287, 341	34000		
8b	269, 311*, 360sh	69000	479	12000
9b	315*, 356sh	69,600	485*, 537sh, 665, 694sh	11100

*denotes λ_{max} and ε_{max} is given

Table S10 UV-Vis absorption properties of M(pherpy)$_2$-2PF$_6$ complexes **3a** – **9a** in methylene chloride

	λ_{max} (nm)	ε_{max}	$\lambda_{maxMLCT}$ (nm)	$\varepsilon_{maxMLCT}$
1	298*, 355	42100		
3a	305*, 367	57000	486, 579*	8000
4a	305*, 360sh	47000		
5a	307*, 351, 371	51000		
6a	306*, 354, 370	56000		
7a	308*, 351, 369	54000		
8a	298*, 333, 365sh	72000	469, 485, 500*	10000
9a	299*, 337sh	57800	505*, 690	9300

*denotes λ_{max} and ε_{max} is given

D) Cyclic Voltammetry

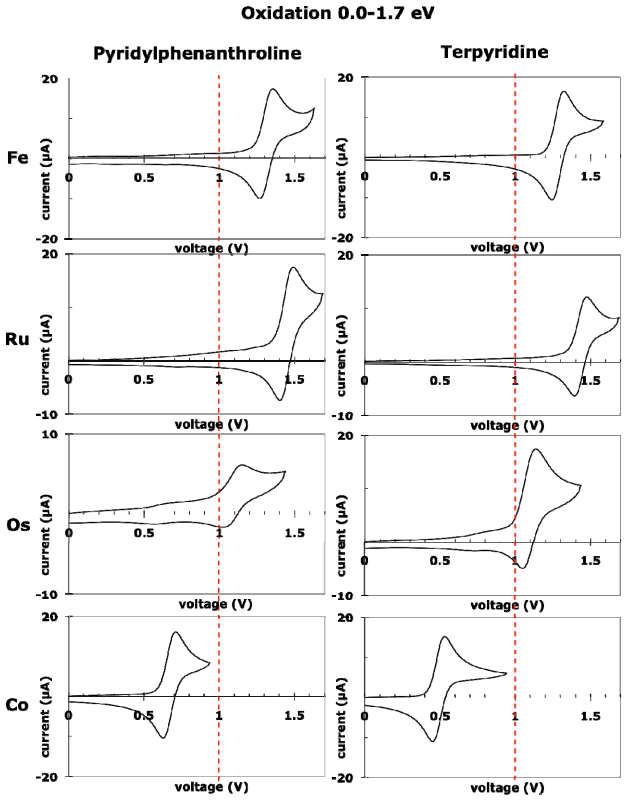

Fig S15. Oxidation voltammetry curves for **3a/b**, **8a/b**, **9a/b** and **4a/b**.

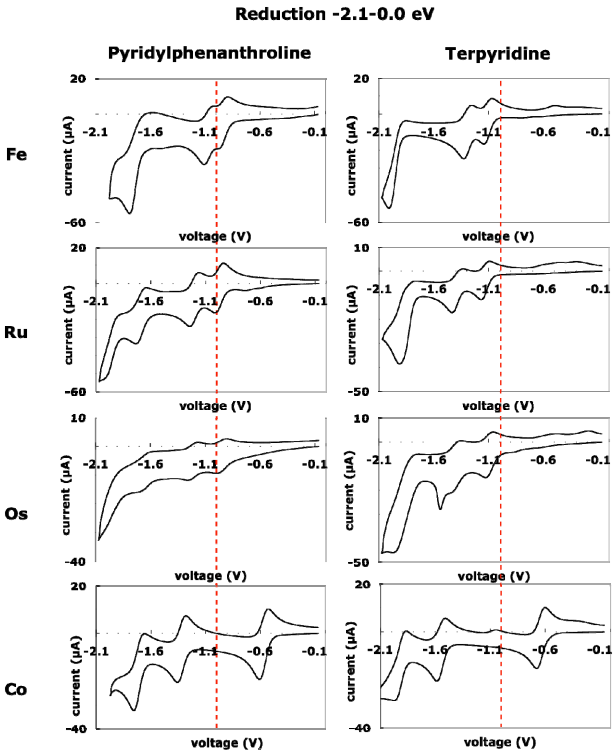

Fig S16. Reduction voltammetry curves for **3a/b**, **8a/b**, **9a/b** and **4a/b**.

Table S12. Redox voltammetry potentials for **3a/b**, **4a/b**, **8a/b** and **9a/b** in acetonitrile, against Ag+/AgCl electrode and referenced to ferrocene as 0.5 eV.

	Oxidation	Reduction1	Reduction 2	Reduction3
3a	1.31	-0.93(s)	-1.06(s)	
3b	1.28	-1.11	-1.29	
4a	0.67	-0.57	-1.32	-1.71
4b	0.49	-0.64	-1.54	-1.92
8a	1.45	-0.98	-1.20	-1.69
8b	1.43	-1.13	-1.40	
9a	1.09	-0.95	-1.21	
9b	1.09	-1.09	-1.40	

*denotes λ_{max} and ε_{max} is given